Avalanche criticality in the martensitic transition of $Cu_{67.64}Zn_{16.71}Al_{15.65}$ shape-memory alloy: A calorimetric and acoustic emission study

María Carmen Gallardo,* Julia Manchado, Francisco Javier Romero, and Jaime del Cerro
Departamento de Física de la Materia Condensada, Universidad de Sevilla, P.O. Box 1065, E-41080 Sevilla, Andalucia, Spain

Ekhard K. H. Salje
Department of Earth Sciences, University of Cambridge, Downing Street, Cambridge CB2 3EQ, United Kingdom

Antoni Planes
Departament d'Estructura i Constituents de la Matèria, Facultat de Física, Universitat de Barcelona, Diagonal 647, E-08028 Barcelona, Catalonia, Spain

Eduard Vives
Department of Physics, University of Warwick, Coventry CV4 7AL, United Kingdom

Ricardo Romero and Marcelo Stipcich
IFIMAT, Universidad del Centro de la Provincia de Buenos Aires, Pinto 399, 7000 Tandil, Argentina
(Received 25 November 2009; revised manuscript received 18 February 2010; published 3 May 2010)

The first-order diffusionless structural transition in $Cu_{67.64}Zn_{16.71}Al_{15.65}$ is characterized by jerky propagation of phase fronts related to the appearance of avalanches. In this paper, we describe a full analysis of this avalanche behavior using calorimetric heat-flux measurements and acoustic emission measurements. Two different propagation modes, namely, smooth front propagation and jerky avalanches, were observed in extremely slow measurements with heating and cooling rates as low as a few 10^{-3} K/h. Avalanches show criticality where each avalanche leads to a spike in the heat flux. Their statistical analysis leads to a power law $[P(E) \sim E^{-\varepsilon}$, where $P(E)dE$ is the probability to observe an avalanche with energy E in an interval between E and $E+dE]$ with an energy exponent of $\varepsilon = 2.15 \pm 0.15$ in excellent agreement with the results of acoustic emission measurements. Avalanches appear to be more common for heating rates faster than 5×10^{-3} K/h whereas smooth front propagation occurs in all calorimetric measurements and (almost) exclusively for slower heating rates. Repeated cooling runs were taken after a waiting time of 1 month (and an intermediate heating run). Correlations between the avalanche sequences of the two cooling runs were found for the strongest avalanche peaks but not for the full sequence of avalanches. The memory effect is hence limited to strong avalanches.

DOI: 10.1103/PhysRevB.81.174102 PACS number(s): 81.30.Kf, 65.40.−b, 64.60.av, 64.60.My

I. INTRODUCTION

The thermodynamic analysis of continuous phase transitions requires thermal fluctuations even when the transitions occur under circumstances in which the mean-field description is not an approximation but strictly correct (such as in ferroelastic transitions). The most direct experimental observation of thermal fluctuations in continuous transitions, relates to the measurements of specific-heat anomalies, which either display critical phenomena[1–5] or mean-field behavior[2,6–9] independently of the nature and the characteristic bonding mechanism of the material. This situation is different in stepwise, first-order transitions where the transition near the interface between the high- and low-temperature phases is riddled with metastable states. If the coexistence interval between the two phases is small, it becomes difficult to explore such metastabilities. Previous work relates mainly to oxides and fluorites with perovskite structure where transitions such as in Ca-doped $KMnF_3$ show essentially a smooth mean-field behavior for both the continuous transitions (high Ca content) and the discontinuous transition (low Ca content).[10–12] It appears that the resolution of experimental techniques is insufficient (so far) to observe metastable states in such systems. On the other hand, when the coexistence interval is large, as in many martensitic shape-memory alloys (SMAs), one observes that the transition behavior is dominated by local transitions between metastable configurations which are not thermally activated.[13–17] The energy landscape is rough and transitions between states can be initiated by changes in conjugated fields such as stress, magnetic fields, electric field, and so forth. If the nonthermal excitations dominate the transition, the transition behavior is termed athermal.[18–21] Athermal phase transformations are much more common phenomenon than just encountered in martensitic phase transformations, they have also been observed in minerals and ceramics.[22–25] While athermal transitions are expected to be a rather common phenomenon, they are also limited to a specific range of external parameters under which they can be observed.[18] We will argue in this paper that the cutoff below which no athermal transitions occur is below a lower limit for the heating/cooling rate ($<5 \times 10^{-3}$ K/h for $Cu_{67.64}Zn_{16.71}Al_{15.65}$) where the transition still progresses but where no avalanches were

found. At higher heating rates, we see spikes in the calorimetric response.

While the observation of specific-heat anomalies is a very common technique in (nearly) second-order phase transitions, the equivalent observations in strongly first-order transition are rather uncommon. The reason is that the observation at fast scanning rates shows large, integrated peaks of the latent heat which mask the underlying fine structure. This fine structure is only seen under relatively slow scanning rates and consists of spikes which relate to sudden transfers between metastable states.[26–29] Even their theoretical description is not much advanced besides the result that such spikes and avalanches are—over a large range in parameter space—critical and that the analysis will follow power-law behavior over 1–3 orders of magnitude. Computer simulations have given some further insight into the character of the metastable states while a full description depends sensitively on the size of the simulated cell.[30–35] In particular, the role of dislocations[17,36] has been invoked to describe the physical origin of avalanches. Recent experimental work on CuAlBe (Ref. 26) showed that dislocations where indeed nucleated during the phase transformation which lead to intense pinning of twin boundaries in the martensitic phase. Avalanches in the elastic response were observed in the coexistence interval while a direct connection of the dislocation density and the transformation mechanism remained elusive.

The importance of heat-flow measurements is that they integrate over all trajectories between metastable states and is, thus, an objective and unbiased observer of all mechanisms which may play a role in the phase transformation. The only limitation is that any measurement of caloric quantities requires that the time needed for the heat flow is short compared with the characteristic time of the phase transformation. This is a trivial requirement in displacive second-order transitions where the characteristic time of the transformation is determined by the soft mode. This situation becomes more complicated in transitions of the order/disorder type where equilibrium states may be obtained only after excessive times.[37] In stepwise transitions we find that the characteristic times for athermal changes can be very long (in fact logarithmically long in spin glasses) but still finite in martensites where the experimentally observed time between larger avalanches is sufficiently long when the transition is thermally driven. This requires that the characteristic time for the experimental observation of avalanches has to be longer than the time required to induce such avalanches. Empirically we have found that avalanche signals do not overlap and still produce measurable signals when the heating/cooling time of the experiment is between 5×10^{-3} and 0.1 K/h. On this time scale, we can distinguish between events which are clearly related to avalanches and those which relate to a smooth background while acoustic emission (AE) experiments analyze the avalanche part only. The intrinsic difficulty, even with calorimetric measurements, remains that very small avalanches could form part of the background so that some of the smooth part of the transition behavior may still contain avalanches which were unresolved experimentally. However, changes in regimes between macroscopically smooth and jagged behavior are clearly observed. It is the purpose of this paper to give the results of heat-flux and acoustic emission measurement of the archetypal shape-memory alloy Cu-Zn-Al.

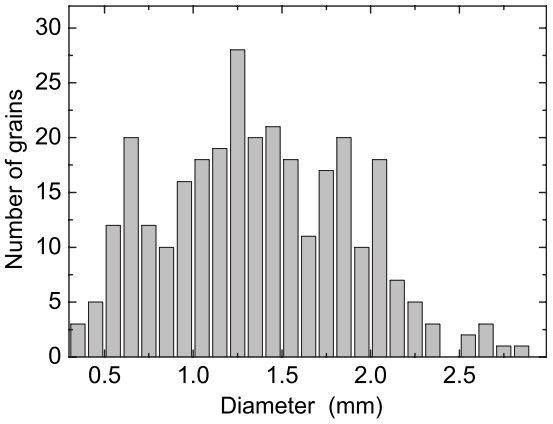

FIG. 1. Grain-size distribution of the sample used for calorimetric and acoustic emission studies. The average grain-size diameter is 1.36 ± 0.03 mm.

II. SAMPLE PREPARATION

The Cu-Zn-Al sample was prepared by alloying 99.99% purity copper, zinc, and aluminum. Small pieces with appropriate masses (weighted with a precision of 0.1 mg) of each metal were cut and melted in a sealed quartz tube under a partial Ar atmosphere in a resistive furnace. The melt was vigorously shaken several times in order to obtain a homogeneous solution. After solidification, the alloy was homogenized at 1073 K for about 4 days and air cooled to room temperature. The nominal composition of the alloy was Cu (67.64 at. %), Zn (16.71 at. %), and Al (15.65 at. %).

The Cu-based SMAs transforms from a high-temperature $L2_1$ ($Fm3m$) structure to several possible martensitic phases, depending on the composition. For this composition, the transition proceeds to a $18R$ ($I2/m$) phase.

From ingots, samples were cut with a low-speed diamond saw. The slices were subjected to an isothermal aging at 1173 K for $\approx$7500 s and subsequently air cooled to room temperature. This heat treatment ensures samples with a highly ordered state, free from internal stresses and with minimum vacancy concentration. Moreover, this heat treatment resulted in a large grain size with average diameter of 1.36 mm (Fig. 1). The sample used in the calorimetric measurements had a flat surface of 0.94 cm^2, a thickness of 0.389 cm, and a mass of 2.6503 g. The sample for AE measurements was much smaller with dimensions of approximately $0.5\times0.5\times0.1$ cm^3 and a mass of 0.185 g.

III. EXPERIMENTAL METHODS

Measurements of heat flux and specific heat were performed using a high-resolution conduction calorimeter, which has been described in detail elsewhere.[38] The sample is pressed between two identical heat-flux meters, which are made from 50 chromel-constantan thermocouples connected in series, with the wires placed in parallel lines.[39] Two electrical resistance heaters are placed near the sample surface

and the flux meter. These heaters dissipate heat uniformly to the sample surface. The assembly is placed in a cylindrical hole located axially in a bronze cylinder (10 kg) which serves as heat sink and constitutes the calorimeter block. The block temperature is measured with a commercial platinum thermometer (Leads and Northrup model 8164B). The block and two surrounding radiation shields are placed into a hermetic outer case under vacuum (10^{-7} torr). The assembly, surrounded by a coiled tube, is placed in a Dewar jar filled with alcohol. The temperature of the alcohol bath is controlled by circulation of liquid N_2 through the coil. A Pt-100 thermometer and a Eurotherm 818 controller are used for the temperature control.

The heat flux is evacuated through the flux meters and allows measurement of heat flux better than 0.1 μW. Due to the high thermal inertial of the calorimetric block, the temperature changes are some 10^{-3} K/h with temperature fluctuations of the calorimeter block smaller than 10^{-6} K.

A long-periodic series of square thermal pulses is superimposed on a heating or cooling ramp. Integration of the electromotive force (emf) given by the flux meters between steady states determines the thermal capacity of the sample.[40]

The equipment also works as a differential thermal analysis (DTA) device. A DTA trace is quasicontinuously measured (12.5 measurements per second) using the same temperature scanning rate as applied during measurement of the specific heat. The emf given by the flux meters is proportional to the heat flux, ϕ_D, the integral with respect to a suitable base line is proportional to the excess enthalpy of the sample.

The value of the latent heat is obtained by integration of ϕ_D/v, where v is the temperature scanning rate, with respect to an appropriate baseline. The sensitivity of this method is estimated to be better than 5 mJ.[41–46]

AE measurements were carried out on a small square sample (dimensions: $5\times5\times1$ mm) cut from the same rod beside the sample used for calorimetric measurements. AE was detected using a piezoelectric transducer, acoustically coupled to the sample. The detected signal was preamplified (40 dB) and monitored by a PCI-2 acquisition system from Euro Physical Acoustics SA, at a sampling rate of 2 M samples per second. A 100 kHz–1 MHz bandwidth filter was used in order to reduce noise. From the recorded signal, individual AE hits were defined by using a threshold of 45 dB. When the signal crosses the threshold a hit starts. When the signal remains below the threshold more than 100 μs the hit ends. This is the so-called hit detection threshold. The system allows a maximum duration of the detected signals of 10 ms. Hits were recorded during cooling and heating ramps between 270 and 215 K at rates in the range 1–0.5 K/min. The typical number of detected events in a ramp was 5000 during cooling and 17 000 during heating. The experimental setup allows the direct measurement of the energy associated with each individual hit by performing a fast integration of the square of the signal. This measurement provides information related to the recorded signals but its relation to the energy released by the source of AE is, *a priori*, not reliably established.

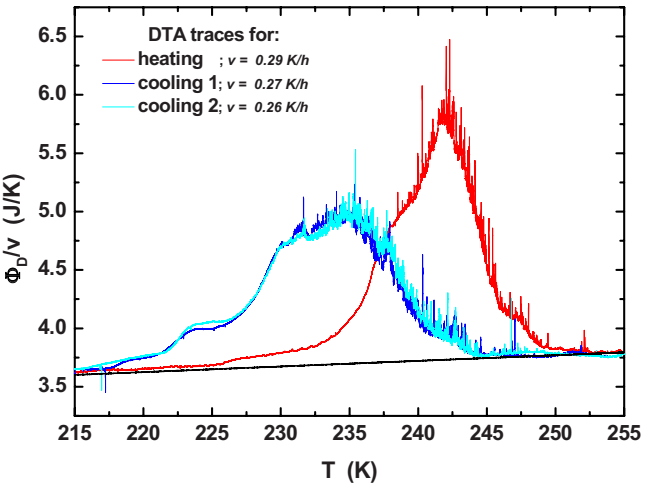

FIG. 2. (Color online) DTA traces for cooling and heating experiments. The heating rate was 0.29 K/h and the cooling rates were 0.27 and 0.26 K/h. Data corresponding to cooling experiments have been changed in sign to allow a better comparison to heating data.

IV. EXPERIMENTAL RESULTS

DTA traces were obtained from heating and cooling runs at a constant rate of ~0.25 K/h (Fig. 2). The second cooling run in Fig. 2 was taken 1 month after the first cooling run and demonstrates that the overall pattern of the transition is fully reproducible. The transition is characterized by a broad, unstructured anomaly of the heat flux between 215 and 255 K together with a large number of spikes over a smaller temperature interval toward the upper end of the smooth anomaly. The detailed analysis of the two cooling runs shows that the larger peaks (>10 μW) appear under exactly the same temperature conditions while smaller peak between the two runs do not correlate. The smooth background is almost identical for the two runs. The spikes of the experiments were extracted after removal of the smooth background and are shown in Fig. 3.

The black solid straight line is an extrapolation of the data obtained at high temperature and it is used to obtain the total enthalpy of the transformation.

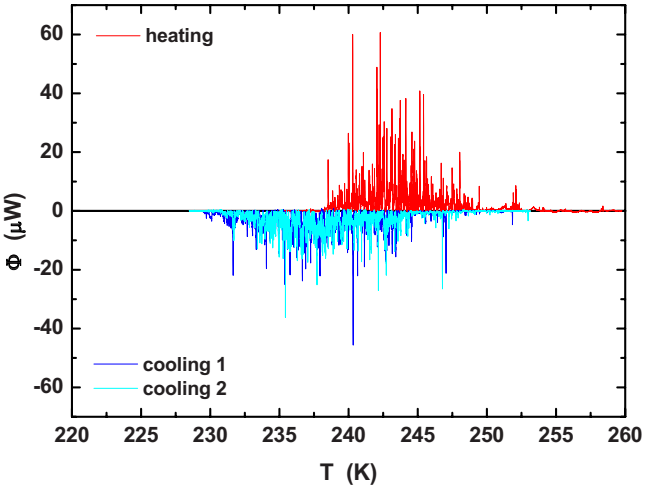

FIG. 3. (Color online) Spikes in the calorimetry measurement after removing the smooth baseline.

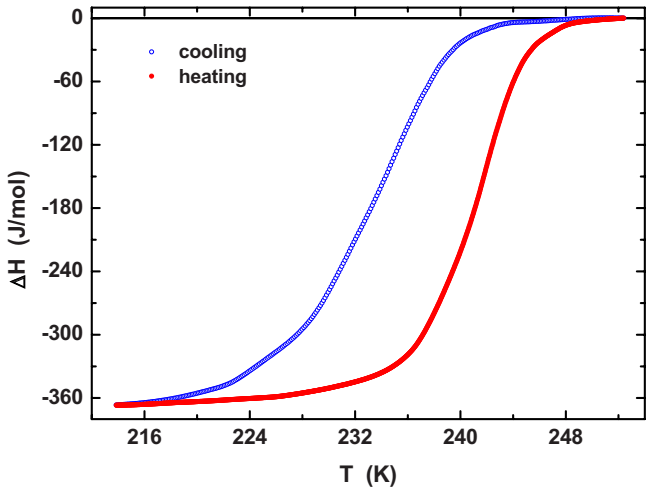

FIG. 4. (Color online) Integrated transition enthalpy for heating and cooling runs. The total enthalpy change is, within experimental errors, identical for heating and cooling experiments.

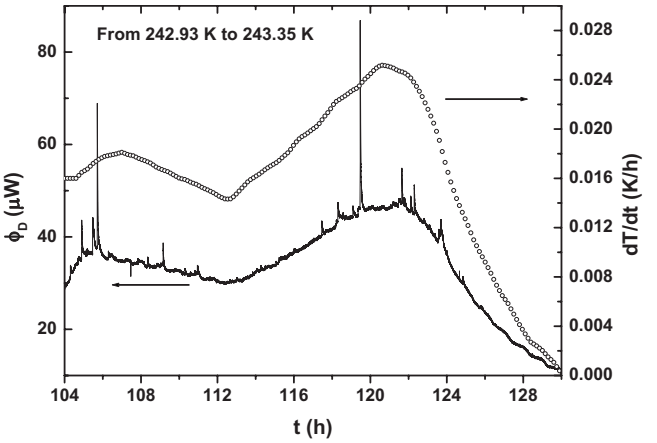

FIG. 5. Traces of rates (upper curve) and heat flux as a function of measurement time. The temperature was practically constant near 243 K and the fluxes are extremely low. No spikes are observed at low fluxes.

Integration of the DTA traces leads to an estimate of the transition enthalpy as shown in Fig. 4. The total transition enthalpy is 370 ± 10 J/mol.

The latent heat has two contributions. The first is related to the smooth background (between $T_1=215$ K and $T_3=253$ K) and the second arises from the spikes observed in the range between $T_2=230$ K (on cooling) and T_3 which are superimposed to the smooth background. It has been estimated that only 10% of the total excess heat in the cooling experiment corresponds to the spikes shown in Fig. 3. In order to analyze carefully the kinetic behavior of the spikes, a new experiment was carried out. During a heating run, the temperature of the thermal bath was fixed at 244 K, within the temperature range where the spikes appear. In a period of 25 h, the temperature of the sample changed from 242.93 to 243.35 K. The heat flux was determined by 12.5 measurements per second and the temperature was measured every 9 min.

In Fig. 5, the heat flux ϕ_D and the temperature variation rate, v, of the calorimeter block (whose temperature practically coincides with that of the sample) are shown as a function of measurement time. Both curves are correlated; the highest density of spikes appears for higher-temperature variation rates. No spikes were found for temperature rates lower than 5×10^{-3} K/h. The effect is seen in more detail in Figs. 6(a) and 6(b), corresponding to enlargements of Fig. 5. In these graphs, the rates are constant [0.024 K/h in (a) and 0.011 K/h in (b)]. The DTA traces show spikes for the faster rate but virtually no spikes for the slower rate.

We now report on the investigation of the phase transformation using the AE technique. Figure 7 shows the AE activity as a function of temperature. The acoustic activity is represented by a histogram giving the number of hits in intervals of 0.04 K.

AE was found in a slightly smaller temperature interval as the spikes in the calorimetric experiments (Fig. 3), where spikes were observed at 230 K. The cooling rate in the AE experiment is faster than in the calorimeter so that the difference of 6 K for the onset of spikes may be due to kinetic effects or a feature of the very different masses of the two samples. Extremely low rates were not used in the AE experiments so that we cannot tell whether the decay of the spikes at very low rates also occurs in AE. These data confirm previous observations.[47]

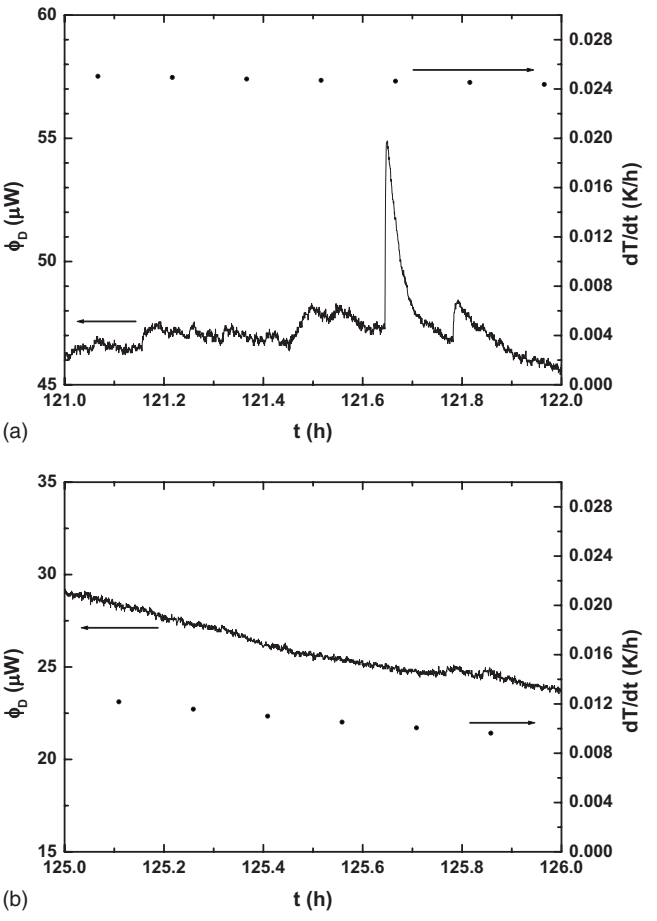

FIG. 6. DTA traces at constant-temperature rates (a) with spikes for the faster rate and (b) no spikes for the slower rate.

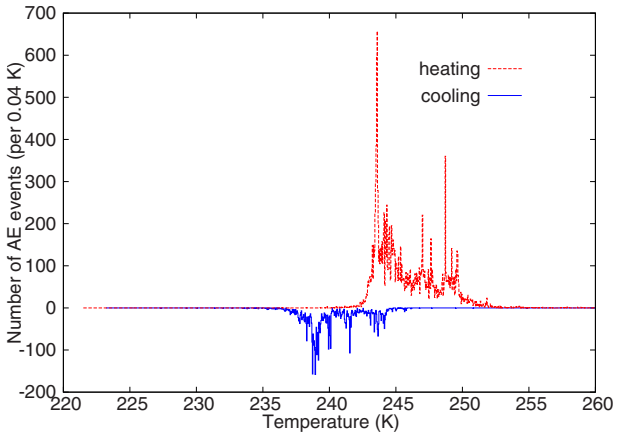

FIG. 7. (Color online) Acoustic emission activity as a function of temperature for the forward and reverse transitions.

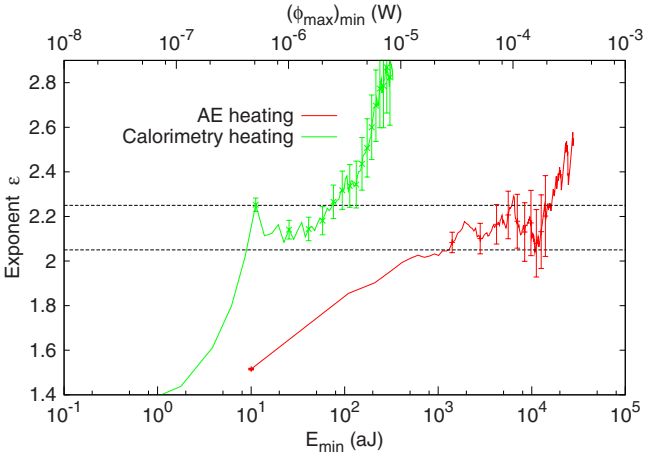

FIG. 8. (Color online) Power-law exponent as a function of integration interval. The optimal exponent lies on the plateau and is $\varepsilon = 2.15 \pm 0.05$ for AE and calorimetric measurements.

V. AVALANCHE STATISTICS

We now turn to the discussion of the statistical analysis of the spikes in the calorimetric and acoustic emission experiments. Inspection of Figs. 3 and 7 already leads to the conclusion that both features have the same physical origin. It is understood that the AE signals record avalanche behavior in $Cu_{67.64}Zn_{16.71}Al_{15.65}$ so that we can assume that avalanches are also at the origin of the spikes in the calorimetric measurements. It needs to be born in mind, however, that avalanches seen in calorimetry are vastly more energetic than those seen in AE. If, as we will show, the statistical analysis is identical for both experimental techniques, it becomes clear that the absolute scales of the avalanche amplitudes differ by several decades so that the full range of the power law extends over several decades while each technique individually covers only about 1–3 decades

The height of each spike was determined with respect to the smooth variation in the background, where the spikes are superimposed. Taking into account that the response of the calorimetric device to a heat-flux pulse in the sample is represented by a single-exponential decay whose time constant is larger than the characteristic time of the avalanches, the height of the peaks is proportional to the energy of each pulse,

$$E = \int_{\Delta t} \phi(t)dt \approx \phi_{max}\Delta t \propto \phi_{max}.$$

In order to obtain the estimation of the power-law exponents, we have performed Maximum Likelihood (ML) fits of a power-law probability density,

$$p(E)dE = \frac{E^{-\varepsilon}dE}{\int_{E_{min}}^{\infty} E^{-\varepsilon}dE},$$

where besides the value of the lower cutoff, the exponent ε is the unique free fit parameter. The expected dependence of ε with the cutoff E_{min} has been studied in detail in Ref. 48. One expects that the exponent increases when the cutoff is increased while a plateau is seen at the best estimation of the exponent. The number of available data is 17 936 for heating AE runs, 4893 for cooling AE runs, 1862 for heating calorimetric run, and 1896 for the cooling calorimetric runs. Figure 8 shows the behavior of the fitted exponent for the calorimetric (left) and AE data (right) corresponding to the heating runs. The value of the cutoff for the calorimetric data, $(\phi_{max})_{min}$, is shown in the scale above and the value of the cutoff for the AE data is shown below.

The behavior is qualitatively similar to the one expected theoretically. Typical error bars are also estimated by the ML analysis. The plateau in both cases is located around a value of the exponent 2.15 and extended in 1 decade. Lines with this slope have been plotted on the histograms in Figs. 9 and 10. Our data agree well with results from a calorimetric study of avalanches during stress-induced martensitic transformation in a $Cu_{67.5}Zn_{19.4}Al_{13.1}$ single crystal, reported in Ref. 49. The paper focused on the effect of cycling on avalanches. In first cycles (following high-temperature annealing and water quench at room temperature), the authors find avalanche criticality. The exponents corresponding to the energies of the avalanches are 1.8 ± 0.3. This value is in rea-

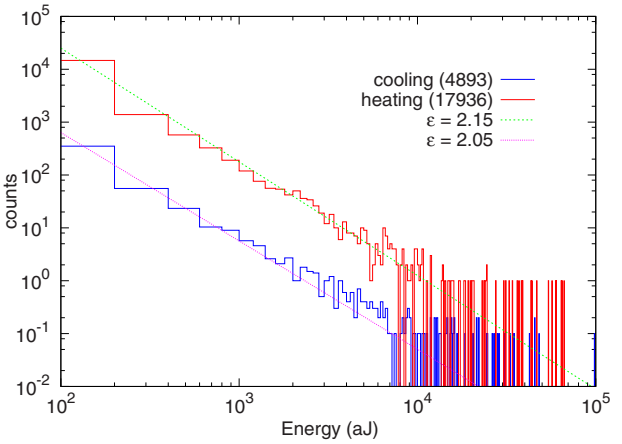

FIG. 9. (Color online) Statistical analysis of the AE observations. Data corresponding to cooling experiments have been shifted 1 decade downward in order to clarify the picture.

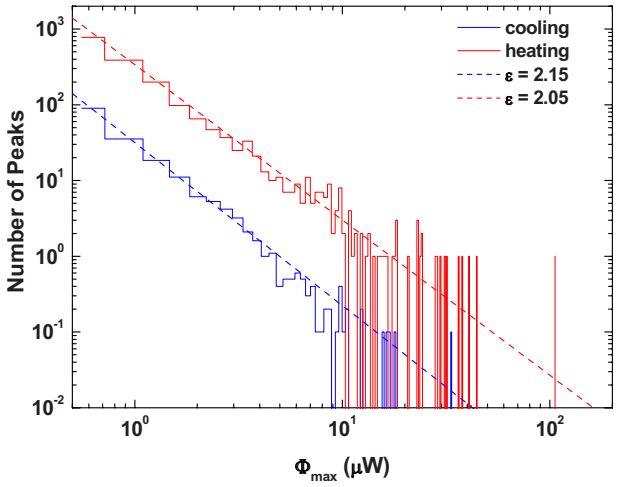

FIG. 10. (Color online) Statistical analysis of the heating and cooling curves of the DTA traces in Fig. 2. Only the distribution of spikes (Fig. 3) is seen in these graphs. Data corresponding to cooling experiments have been shifted 1 decade downward in order to clarify the picture.

sonable agreement with our present estimations.

It has been shown previously that the value of the exponents depends not only on the symmetry of the martensitic phase but also on the individual compound or any chemical specificity. This argument reinforces the hypothesis of universality of the exponents in avalanche criticality.[18] It is important to notice that the relatively large scatter of the data in the literature is due to the rate dependence of the exponents. Actually, the true universal value corresponds to the adiabatic limiting value which is approached in our experiments. We conclude this discussion with the observation that avalanches can be measured quantitatively in calorimetric experiments provided that the change in temperature during the experiment is sufficiently slow.

VI. "CONTINUOUS" HEAT FLUX

We now turn to the description of the smooth part of the DTA curves in Fig. 2, i.e., those enthalpic changes where significant avalanche contribution, such as shown in Fig. 3, are small or do not exist. In this context, it is irrelevant whether small avalanches are still hidden inside the enthalpic change, the crux of the matter is that the statistics of the transformation mechanism changes dramatically. It is also significant that previous experimental results[47] did show some smooth background in AE while our present results showed no AE activity between 216 and 235 K where the calorimetric changes are significant. Let us remind ourselves that AE originates from the sudden progression of interfaces so that the change in statistics can be discussed in terms of interface propagation. In fact, the change in progression of interfaces is well known for the dynamics of twin boundaries in ferroelastic and ferroelectric materials when external force fields are applied. Newton's law would require that the movement of interfaces under stress or electric fields has to be accelerated. Experimentally, this is never the case, in fact all experimental observations show that the movement of the interface is momentum driven, i.e., the interfaces propagate with constant speed which is equivalent to the solution of the dynamic equation of an over damped system with no effective mass.[7] The physical reason for this behavior is related to the dissipation of energy during the interfacial movement either via phonons or via defects where acceleration over small distances is brought to a standstill by defect pinning. The wall then unpins either thermally or via the external force, accelerates again, and gets again pinned. This stop-and-go mechanism leads to macroscopically over damped, smooth propagation of the interface (while "smoothness" does not necessarily exist on an atomic level when extrinsic defects are present). The same smooth behavior can be attributed to the smooth enthalpic change seen in our experiments. In terms of the avalanche statistics, this would mean that the average propagation distance of the phase front becomes comparable with the distance of pinning centers.[50–54]

The same multiscaling argument can also be applied to the behavior of the macroscopic Gibbs free energy of the phase transformation. Let us consider the behavior of the virgin crystal as a first-order transition with a Landau potential as in NiTiFe.[21] We then expect the latent heat to be released inside the coexistence interval. Slow heating and cooling experiments will change the microstructure and the pinning behavior, however. This effect may lead to a local variation in the transition temperature well over and above the coexistence interval (see local temperature approximation[55]). In stress-driven transitions,[56] the transition temperature becomes an explicit function of stress. Compactification then leads to a macroscopic behavior which is smooth with a steep decay of the order parameter in the martensitic phase before the coexistence interval is reached while heating.[7]

Finally, we speculate on the limiting case of isothermal transitions in the limiting case of vanishing heating or cooling rates. Our experiments with cooling rates below 5×10^{-3} K/h seem to imply that all fronts propagate smoothly while avalanches are seen only for faster rates. The experiment was performed in a temperature regime where avalanches are particularly plentiful so that we may be able to extrapolate these data for the entire coexistence range. This observation is in basic agreement with the idea that phase fronts require defects to become jerky and form avalanches. When the relaxation time of the defects or their time to diffuse with the phase front becomes comparable with the characteristic time of the front propagation, one would not expect avalanches to occur. This may be exactly the case of our "slow" experiment and is in full agreement with previous observations in ferroelastic materials that slow elastic responses of crystals show the diffusion rate of the defects while fast responses show pinning of the interfaces by walls. If this interpretation is correct in case of $Cu_{67.64}Zn_{16.71}Al_{15.65}$, it provides the rough estimate for the relaxation time of pinning centers. We take as the temperature jump required to move a phase front as 10^{-3} K and the limiting rate of 10^{-3} K/h, we obtain a characteristic time of 4×10^{8} s. The average distance between pinning centers may be guessed to be 10^{-8} m so that the diffusion coefficient has the order of magnitude of 10^{-24} m/s^2 which is in the correct order for

self diffusion of Ti in TiAl.[57] This would indicate that very slow movement of interfaces may, in fact, eliminate the occurrence of avalanches in $Cu_{67.64}Zn_{16.71}Al_{15.65}$.

ACKNOWLEDGMENTS

The calorimetric experiments have been supported in Seville by CICyT (Spain) under Project FIS2006-04045. J. Manchado wishes to thank Fundación Cámara for a research grant. We also want to thank J. Jiménez for his help in supporting the experimental system and J. M. Martín-Olalla for fruitful discussions in the calculation of power-law distributions. The work in Barcelona received financial support from CICyT (Spain) under Project No. MAT 2007-61200.

*mcgallar@us.es

[1] R. Bausch, H. K. Janssen, and H. Wagner, Z. Phys. B **24**, 113 (1976).
[2] A. Pelissetto and E. Vicari, Phys. Rep. **368**, 549 (2002).
[3] A. Vespignani and S. Zapperi, Phys. Rev. E **57**, 6345 (1998).
[4] L. F. Cugliandolo and J. Kurchan, J. Phys. A **27**, 5749 (1994).
[5] J. P. Sethna, K. Dahmen, S. Kartha, J. A. Krumhansl, B. W. Roberts, and J. D. Shore, Phys. Rev. Lett. **70**, 3347 (1993).
[6] E. K. H. Salje, B. Wruck, and H. Thomas, Z. Phys. B: Condens. Matter **82**, 399 (1991).
[7] E. K. H. Salje, *Phase Transitions in Ferroelastic and Co-elastic Crystals*, 2nd ed. (Cambridge University Press, Cambridge, UK, 1993); M. A. Carpenter, E. K. H. Salje, and A. Graeme-Barber, Eur. J. Mineral. **10**, 621 (1998).
[8] E. K. H. Salje, M. C. Gallardo, J. Jiménez, F. J. Romero, and J. del Cerro, J. Phys.: Condens. Matter **10**, 5535 (1998); S. A. Hayward, F. D. Morrison, S. A. T. Redfern, E. K. H. Salje, J. F. Scott, K. S. Knight, S. Tarantino, A. M. Glazer, V. Shuvaeva, P. Daniel, M. Zhang, and M. A. Carpenter, Phys. Rev. B **72**, 054110 (2005).
[9] J. C. Lashley, S. M. Shapiro, B. L. Winn, C. P. Opeil, M. E. Manley, A. Alatas, W. Ratcliff, T. Park, R. A. Fisher, B. Mihaila, P. Riseborough, E. K. H. Salje, and J. L. Smith, Phys. Rev. Lett. **101**, 135703 (2008).
[10] E. K. H. Salje, M. Zhang, and H. L. Zhang, J. Phys.: Condens. Matter **21**, 335402 (2009).
[11] F. J. Romero, M. C. Gallardo, S. A. Hayward, J. Jiménez, J. del Cerro, and E. K. H. Salje, J. Phys.: Condens. Matter **16**, 2879 (2004).
[12] E. K. H. Salje and H. L. Zhang, J. Phys.: Condens. Matter **21**, 035901 (2009); W. Schranz, P. Sondergeld, A. V. Kityk, and E. K. H. Salje, Phys. Rev. B **80**, 094110 (2009).
[13] *Shape Memory Alloys*, edited by K. Otsuka and C. M. Wayman (Cambridge University Press, Cambridge, UK, 1998).
[14] S. Sreekala, R. Ahluwalia, and G. Ananthakrishna, Phys. Rev. B **70**, 224105 (2004).
[15] E. Vives, J. Ortin, L. Manosa, I. Rafols, R. Pérez-Magrane, and A. Planes, Phys. Rev. Lett. **72**, 1694 (1994).
[16] A. Magni, G. Durin, S. Zapperi, and J. P. Sethna, J. Stat. Mech.: Theory Exp. (2009) P01020.
[17] F.-J. Pérez-Reche, M. Stipcich, E. Vives, L. Mañosa, A. Planes, and M. Morin, Phys. Rev. B **69**, 064101 (2004).
[18] F. J. Pérez-Reche, E. Vives, L. Mañosa, and A. Planes, Phys. Rev. Lett. **87**, 195701 (2001).
[19] F.-J. Pérez-Reche, B. Tadic, L. Mañosa, A. Planes, and E. Vives, Phys. Rev. Lett. **93**, 195701 (2004).
[20] J. E. Martin, R. A. Anderson, and C. P. Tigges, J. Chem. Phys. **108**, 3765 (1998).
[21] E. K. H. Salje, H. Zhang, A. Planes, and X. Moya, J. Phys.: Condens. Matter **20**, 275216 (2008); E. K. H. Salje, H. Zhang, D. Schryvers, and B. Bartova, Appl. Phys. Lett. **90**, 221903 (2007).
[22] H. Zhang, E. K. H. Salje, D. Schryvers, and B. Bartova, J. Phys.: Condens. Matter **20**, 055220 (2008).
[23] U. Sarı, E. Güler, T. Kırındı, and M. Dikici, J. Phys. Chem. Solids **70**, 1226 (2009).
[24] M. Dijkstra, D. Frenkel, and J. P. Hansen, J. Chem. Phys. **101**, 3179 (1994).
[25] C. R. S. Da Silva, B. B. Karki, L. Stixrude, and R. M. Wentzcovitch, Geophys. Res. Lett. **26**, 943 (1999); T. Tsuchiya, J. Tsuchiya, K. Umemoto, and R. M. Wentzcovitch, *ibid.* **31**, L14603 (2004).
[26] E. K. H. Salje, H. Zhang, H. Idrissi, D. Schryvers, M. A. Carpenter, X. Moya, and A. Planes, Phys. Rev. B **80**, 134114 (2009).
[27] E. K. H. Salje, J. Koppensteiner, M. Reinecker, W. Schranz, and A. Planes, Appl. Phys. Lett. **95**, 231908 (2009).
[28] J. M. Delgado-Sánchez, J. M. Martín-Olalla, M. C. Gallardo, S. Ramos, M. Koralewski, and J. del Cerro, J. Phys.: Condens. Matter **17**, 2645 (2005).
[29] S. A. Hayward, F. J. Romero, M. C. Gallardo, J. del Cerro, A. Gibaud, and E. K. H. Salje, J. Phys.: Condens. Matter **12**, 1133 (2000).
[30] D. Sherrington, in *Statistical Physics, High Energy, Condensed Matter and Mathematical Physics*, edited by M.-L. Ge, C. H. Oh, and K. K. Phua (World Scientific, Singapore, 2008), p. 218; E. K. H. Salje, Phys. Chem. Miner. **15**, 336 (1988); E. Salje and K. Parlinski, Supercond. Sci. Technol. **4**, 93 (1991).
[31] K. Binder and J. D. Reger, Adv. Phys. **41**, 547 (1992).
[32] J. R. L. de Almeida and D. J. Thouless, J. Phys. A **11**, 983 (1978).
[33] F. Ritort and P. Sollich, Adv. Phys. **52**, 219 (2003).
[34] J. P. Sethna, K. A. Dahmen, and C. R. Myers, Nature (London) **410**, 242 (2001).
[35] P. Lloveras, T. Castan, M. Porta, A. Planes, and A. Saxena, Phys. Rev. B **80**, 054107 (2009).
[36] F.-J. Pérez-Reche, L. Truskinovsky, and G. Zanzotto, Phys. Rev. Lett. **101**, 230601 (2008).
[37] M. Zhang, B. Wruck, A. G. Barber, E. K. H. Salje, and M. A. Carpenter, Am. Mineral. **81**, 92 (1996).
[38] M. C. Gallardo, J. Jiménez, and J. del Cerro, Rev. Sci. Instrum. **66**, 5288 (1995).
[39] J. Jiménez, E. Rojas, and M. Zamora, J. Appl. Phys. **56**, 3353 (1984).
[40] J. del Cerro, J. Therm. Anal. **34**, 335 (1988).
[41] J. del Cerro, J. M. Martín-Olalla, and F. J. Romero, Thermochim.

Acta **401**, 149 (2003).
[42] J. del Cerro, F. J. Romero, M. C. Gallardo, S. A. Hayward, and J. Jiménez, Thermochim. Acta **343**, 89 (2000).
[43] F. J. Romero, M. C. Gallardo, A. Czarnecka, M. Koralewski, and J. Del Cerro, J. Therm. Anal. Calorim. **87**, 355 (2007).
[44] F. J. Romero, M. C. Gallardo, J. Jiménez, A. Czarnecka, M. Koralewski, and J. del Cerro, J. Phys.: Condens. Matter **16**, 7637 (2004).
[45] J. Manchado, F. J. Romero, M. C. Gallardo, J. del Cerro, T. W. Darling, P. A. Taylor, A. Buckley, and M. A. Carpenter, J. Phys.: Condens. Matter **21**, 295903 (2009).
[46] F. J. Romero, J. Jiménez, and J. del Cerro, J. Magn. Magn. Mater. **280**, 257 (2004).
[47] A. Planes, J. L. Macqueron, M. Morin, and G. Guenin, Phys. Status Solidi A **66**, 717 (1981).
[48] A. Clauset, C. Rohilla-Shalizi, and M. E. J. Newman, SIAM Rev. **51**, 661 (2009).
[49] L. Carrillo and J. Ortín, Phys. Rev. B **56**, 11508 (1997).
[50] S. A. Hayward and E. K. H. Salje, Am. Mineral. **81**, 1332 (1996); E. K. H. Salje, Eur. J. Mineral. **7**, 791 (1995); E. K. H. Salje, U. Bismayer, B. Wruck, and J. Hensler, Phase Transitions **35**, 61 (1991).
[51] Q. Bronchart, Y. Le Bouar, and A. Finel, Phys. Rev. Lett. **100**, 015702 (2008); D. Rodney, Y. Le Bouar, and A. Finel, Acta Mater. **51**, 17 (2003).
[52] V. Lecomte, S. E. Barnes, J. P. Eckmann, and T. Giamarchi, Phys. Rev. B **80**, 054413 (2009).
[53] Q. Pang, J. M. Zhang, K. W. Xu, and V. Ji, Appl. Surf. Sci. **255**, 8145 (2009); L. Goncalves-Ferreira, S. A. T. Redfern, E. Artacho, and E. K. H. Salje, Phys. Rev. Lett. **101**, 097602 (2008); E. K. H. Salje and H. L. Zhang, Phase Transitions **82**, 452 (2009); K. R. Locherer, S. A. Hayward, P. J. Hirst, J. Chrosch, M. Yeadon, J. S. Abell, and E. K. H. Salje, Philos. Trans. R. Soc. London, Ser. A **354**, 2815 (1996).
[54] A. Agronin, Y. Rosenwaks, and G. Rosenman, Appl. Phys. Lett. **88**, 072911 (2006).
[55] M. A. Krivoglaz, Sov. Phys. JETP **21**, 204 (1965).
[56] E. K. H. Salje, Phys. Rep. **215**, 49 (1992); E. Bonnot, E. Vives, L. Manosa, A. Planes, and R. Romero, Phys. Rev. B **78**, 094104 (2008).
[57] C. Herzig, T. Przeorski, and Y. Mishin, Intermetallics **7**, 389 (1999).